South East Asian J. of Mathematics and Mathematical Sciences
Vol. 18, No. 1 (2022), pp. 147-158

ISSN (Online): 2582-0850

ISSN (Print): 0972-7752

AN EFFICIENT FRACTIONAL INTEGRATION OPERATIONAL MATRIX OF THE CHEBYSHEV WAVELETS AND ITS APPLICATIONS FOR MULTI-ORDER FRACTIONAL DIFFERENTIAL EQUATIONS

R. Aruldoss and R. Anusuya Devi

Department of Mathematics,
Government Arts College (Autonomous),
Kumbakonam - 612002, Tamil Nadu, INDIA

E-mail : krvarul@gmail.com, anushya3sai@gmail.com

(**Received:** *Jan. 05, 2021* **Accepted:** *Feb. 02, 2022* **Published:** *Apr. 30, 2022)*

Abstract: In this paper, a new fractional integration operational matrix of the Chebyshev Wavelets is derived and is used to solve multi-order fractional differential equations. The greater advantage behind the proposed matrix is that any fractional differential equation is reduced into a system of algebraic equations. We show the simplicity, the efficiency and the appropriateness of the proposed technique with some numerical examples.

Keywords and Phrases: Fractional derivatives and integrals, Chebyshev wavelets, Fractional differential equations, Operational matrix.

2020 Mathematics Subject Classification: 26A33, 34A08.

1. Introduction

Fractional differential equations are effectively used in mathematical modelling of many present marvels such as dynamical systems [3], optimal control problems [7], diffusion processes [5] and chaotic systems [12]. Owing to the difficulty of finding exact solutions for many fractional differential equations, several numerical methods are employed, such as Adomian decomposition method [11], Variational iteration method [17], Homotopy Analysis Method [4], Homotopy Perturbation Method [8] and so on.

In the past few decades, wavelet theory has been one of the growing and preponderant methods in the area of mathematical and engineering sciences. In particular, it is used in signal analysis, time-frequency analysis and fast algorithms for easy implementation [1]. Recently, the operational matrices of fractional order integrations of various wavelets, such as Haar wavelets, Legendre wavelets, Bernoulli wavelets, CAS wavelets, Euler wavelets [2, 9, 14, 15, 16] have been established to solve many fractional differential equations. Though each numerical method has its own favourable circumstances, restrictions and constraints, wavelet transform gives a better spectral localization using multiresolution analysis.

In this paper, first we investigate the Cheybyshev wavelets and then we find the operational matrix of fractional order integration of Chebyshev wavelets to solve multi order fractional differential equations. Though, the operational matrix for Chebyshev wavelets is structurally sparse, it decreases greatly the computational complexity of the resulting algebraic system.

The rest of the paper is organized as follows. In Section 2, some basic definitions of fractional calculus are briefly reviewed. Section 3 concerns Chebyshev wavelets. Section 4 deals with function approximation by Chebyshev wavelets. In Section 5, the fractional integration operational matrix of Chebyshev wavelets is obtained. Finally, we apply the proposed technique on solving some multi-order fractional differential equations in Section 6.

2. Preliminaries

In this section, some fundamental definitions of fractional calculus are briefly discussed.

Definition 2.1. *The Riemann-Liouville fractional integral I^γ of order $\gamma \geq 0$ for a function $g(t) \in L^1[0,\infty)$ is defined as*

$$(I^\gamma g)(t) = \begin{cases} \frac{1}{\Gamma(\gamma)} \int_0^t (t-\zeta)^{\gamma-1} g(\zeta) d\zeta, & \gamma > 0, \\ g(t), & \gamma = 0. \end{cases}$$

Moreover, if $g(t) \in L^1[0,\infty)$, $\alpha, \beta, a \geq 0$ and $\gamma \geq -1$, then $(I^\alpha I^\beta g)(t) = (I^\beta I^\alpha g)(t) = (I^{\alpha+\beta} g)(t)$ and $I^\alpha (t-a)^\gamma = \frac{\Gamma(\gamma+1)}{\Gamma(\alpha+\gamma+1)}(t-a)^{\alpha+\gamma}$.

Definition 2.2. *The fractional differential operator of order $\gamma \geq 0$ in the Caputo sense for a function $g(t) \in L^1[0,\infty)$ is defined as*

$$D^\gamma g(t) = \begin{cases} g^{(m)}(t), & \gamma = m \in \mathbb{N}, \\ \frac{1}{\Gamma(m-\gamma)} \int_0^t \frac{g^{(m)}(\zeta)}{(t-\zeta)^{\gamma+1-m}} d\zeta, & m-1 < \gamma < m. \end{cases}$$

If $g(t) \in L^1[0,\infty)$ *and* $\gamma \geq 0$, *then* $(D^\gamma I^\gamma)g(t) = g(t)$ *and*

$$(I^\gamma D^\gamma)g(t) = g(t) - \sum_{l=0}^{m-1} g^{(l)}(0^+)\frac{t^l}{l!}, \quad (m-1 < \gamma \leq m),$$

where $m \in \mathbb{N}$ *and* $g^{(l)}(0^+) := lim_{t\to 0^+} D^l g(t)$.

3. The Chebyshev Wavelets

Wavelets establish a family of functions developed from dilations and translations of a single function $\Psi(t)$, called the mother wavelet. By changing the dilation parameter c and the translation parameter d continuously, we can obtain the following continuous family of wavelets,

$$\psi_{cd}(t) = |c|^{-\frac{1}{2}}\psi\left(\frac{t-d}{c}\right), \; c \neq 0, \; d \in \mathbb{R}.$$

If the translation and dilation parameters are chosen to have discrete values $c = {c_0}^{-j}$, $d = md_0{c_0}^{-j}$, $c_0 > 1$, $d_0 > 0$, $j, m \in \mathbb{Z}$, then we have the following discrete family of wavelets,

$$\psi_{jm}(t) = |c_0|^{\frac{j}{2}}\psi({c_0}^j t - md_0),$$

where the functions ψ_{jm} form a wavelet basis for $L^2[0,\infty)$. In particular, when $c_0 = 2$ *and* $d_0 = 1$, the functions $\psi_{jm}(t)$ form an orthonormal basis.
A family of Chebyshev wavelets over the interval [0,1) is defined by

$$\psi_{mn}(t) = \begin{cases} 2^{\frac{j}{2}}\widetilde{U_n}(2^j t - 2m + 1), & \frac{m-1}{2^{j-1}} \leq t < \frac{m}{2^{j-1}}, \\ 0, & otherwise, \end{cases}$$

where $m = 1, 2, ..., 2^{j-1}, n = 0, 1, ..., M-1, j, M \in \mathbb{N}, \widetilde{U_n}(t) = \dfrac{1}{\sqrt{\pi}}U_n(t)$ and $U_n(t)$'s denote the Chebyshev polynomials of third kind of degree n, which are mutually orthogonal with respect to the weight function $\omega(t) = \frac{\sqrt{(1+t)}}{\sqrt{(1-t)}}$ on the interval [-1,1] and satisfy the following recursive formula $U_0(t) = 1, U_1(t) = 2t - 1, U_{n+1}(t) = 2tU_n(t) - U_{n-1}(t)$.

4. Function Approximation

The Chebyshev wavelets can be used to expand any function $f(t) \in L^2[0,1)$ as

$$f(t) = \sum_{m=0}^{\infty}\sum_{n=0}^{\infty} d_{mn}\psi_{mn}(t), \tag{1}$$

where $d_{mn} =< f(t), \psi_{mn}(t) >= \int_0^1 f(t)\psi_{mn}(t)\omega_m(t)dt$, and $< ... >$ denotes the inner product on $L^2_{\omega_m}[0,1)$.
By truncating the infinite series in (1), $f(t)$ is approximated as

$$f(t) \approx \sum_{m=1}^{2^{j-1}} \sum_{n=0}^{M-1} a_{mn}\psi_{mn}(t) = A^T\Psi(t), \tag{2}$$

where A and $\Psi(t)$ are $2^{j-1}M \times 1$ matrices, given by

$$A = [a_{10}, a_{11}, ..., a_{1(M-1)}, a_{20}, ..., a_{2(M-1)}, ..., a_{2^{j-1}0}, ..., a_{2^{j-1}(M-1)}]^T \text{ and} \tag{3}$$

$$\Psi(t) = [\psi_{10}, \psi_{11}, ..., \psi_{1(M-1)}, \psi_{20}, ..., \psi_{2(M-1)}, ..., \psi_{2^{j-1}(M-1)}]^T. \tag{4}$$

We define the Chebyshev wavelet matrix $\phi_{\widehat{n}\times\widehat{n}}$ at the collocation points

$t_i = \dfrac{2i-1}{2^jM}, i = 1, 2, ..., 2^{j-1}M$ as $\phi_{\widehat{n}\times\widehat{n}} = \left[\Psi\left(\dfrac{1}{2\widehat{n}}\right), \Psi\left(\dfrac{3}{2\widehat{n}}\right), ..., \Psi\left(\dfrac{2\widehat{n}-1}{2\widehat{n}}\right)\right]$,

where $\widehat{n} = 2^{j-1}M$. Specifically, for $j = 2$ and $M = 3$, the Chebyshev wavelet matrix becomes

$$\phi_{6\times 6} = \begin{pmatrix} 1.1284 & 1.1284 & 1.1284 & 0 & 0 & 0 \\ -2.6329 & -1.1284 & 0.3761 & 0 & 0 & 0 \\ 2.3821 & -1.1284 & -0.6269 & 0 & 0 & 0 \\ 0 & 0 & 0 & 1.1284 & 1.1284 & 1.1284 \\ 0 & 0 & 0 & -2.6329 & -1.1284 & 0.3761 \\ 0 & 0 & 0 & 2.3821 & -1.1284 & -0.6269 \end{pmatrix}.$$

5. The Chebyshev wavelet Operational matrix of fractional integration

In this section, we explore the basic idea of finding the fractional integration operational matrix of the Chebyshev wavelets.
An $\widehat{n}$ set of Block pulse functions(BPFs) is defined as

$$b_i(t) = \begin{cases} 1, & (i-1)/\widehat{n} \le t < i/\widehat{n}, \\ 0, & otherwise, \end{cases} \quad \text{where } i = 1, 2, 3, ..., \widehat{n}.$$

For $t \in [0,1)$, $b_i(t)b_j(t) = \begin{cases} 0, & i \neq j, \\ b_i(t), & i = j, \end{cases}$ and $\int_0^1 b_i(\tau)b_j(\tau)d\tau = \begin{cases} 0, & i \neq j, \\ \frac{1}{\widehat{n}}, & i = j. \end{cases}$

Any function $f(t) \in L^2[0,1)$ can be expanded in terms of $\widehat{n}$ set of BPFs as $f(t) = \sum_{i=1}^{\widehat{n}} f_i b_i(t) = f^T B_{\widehat{n}}(t)$, where

$$f = [f_1, f_2, ..., f_{\widehat{n}}]^T, f_i = \frac{1}{\widehat{n}} \int_{(i-1)/\widehat{n}}^{i/\widehat{n}} f(t) b_i(t) dt \text{ and } B_{\widehat{n}}(t) = [b_1(t), b_2(t), ..., b_{\widehat{n}}(t)]^T.$$

The Chebyshev wavelet matrix can be expressed as

$$\Psi(t) = \phi_{\widehat{n}\times\widehat{n}} B_{\widehat{n}}(t). \tag{5}$$

The block pulse operational matrix F^β of fractional integration I^β is defined as in [10], that is,

$$(I^\beta B_{\widehat{n}})(t) \approx F^\beta B_{\widehat{n}}(t), \tag{6}$$

where

$$F^\beta = \frac{1}{\widehat{n}^\beta} \frac{1}{\Gamma(\beta+2)} \begin{pmatrix} 1 & \zeta_1 & \zeta_2 & \zeta_3 & \dots & \zeta_{\widehat{n}-1} \\ 0 & 1 & \zeta_1 & \zeta_2 & \dots & \zeta_{\widehat{n}-2} \\ 0 & 0 & 1 & \zeta_1 & \dots & \zeta_{\widehat{n}-3} \\ \vdots & \vdots & \ddots & \ddots & \vdots & \vdots \\ 0 & 0 & \dots & 0 & 1 & \zeta_1 \\ 0 & 0 & \dots & 0 & 0 & 1 \end{pmatrix},$$

with

$$\xi_j = (j+1)^{\beta+1} - 2j^{\beta+1} + (j-1)^{\beta+1}.$$

The fractional integration of order $\beta \geq 0$ of the vector $\Psi(t)$ defined in (4) can be expressed as

$$(I^\beta \Psi)(t) \approx P^\beta_{\widehat{n}\times\widehat{n}} \Psi(t), \tag{7}$$

where $P^\beta_{\widehat{n}\times\widehat{n}}$ is called the Chebyshev wavelet operational matrix of order $\beta \geq 0$. Using (5) and (6), we obtain,

$$(I^\beta \Psi)(t) \approx (I^\beta \phi_{\widehat{n}\times\widehat{n}} B_{\widehat{n}})(t) = \phi_{\widehat{n}\times\widehat{n}} (I^\beta B_{\widehat{n}})(t) \approx \phi_{\widehat{n}.\times\widehat{n}} F^\beta B_{\widehat{n}}(t) \tag{8}$$

Moreover, from (7) and (8), we have

$$P^\beta_{\widehat{n}\times\widehat{n}} \Psi(t) \approx (I^\beta \Psi)(t) \approx \phi_{\widehat{n}\times\widehat{n}} F^\beta B_{\widehat{n}}(t). \tag{9}$$

Thus by considering (5) and (9), we attain

$$P^\beta_{\widehat{n}\times\widehat{n}} \approx \phi_{\widehat{n}\times\widehat{n}} F^\beta \phi^{-1}_{\widehat{n}\times\widehat{n}}. \tag{10}$$

In particular, the Chebyshev wavelet operational matrix of the fractional integration for $j = 2, M = 3$ and $\beta = 0.5$ yields

$$P^{0.5}_{6\times 6} = \begin{pmatrix} 0.6691 & 0.1325 & -0.0250 & 0.3827 & -0.0539 & 0.0215 \\ -0.5266 & 0.2205 & 0.1537 & -0.3226 & 0.0282 & -0.0023 \\ 0.0221 & -0.2396 & 0.0318 & 0.0194 & 0.0104 & -0.0091 \\ 0 & 0 & 0 & 0.6691 & 0.1325 & -0.0250 \\ 0 & 0 & 0 & -0.5266 & 0.2205 & 0.1537 \\ 0 & 0 & 0 & 0.0221 & -0.2396 & 0.0318 \end{pmatrix}.$$

As $P^{\beta}_{\widehat{n}\times\widehat{n}}$ contains many zeros, the proposed technique will have faster simulations. $P^{\beta}_{\widehat{n}\times\widehat{n}}$ is done once and is utilized to solve fractional order differential equations just as integer order differential equations.

6. Numerical Examples

In this section, some numerical examples are given to illustrate the efficiency and the reliability of the proposed technique and all the numerical calculations are performed by MATLAB.

Example 6.1. Consider the multi-order fractional differential equation [6]

$$D^{\gamma}u(t) = y_0 D^{\gamma_0}u(t) + y_1 D^{\gamma_1}u(t) + y_2 D^{\gamma_2}u(t) + y_3 D^{\gamma_3}u(t) + f(t), \quad t \in [0, 1), \tag{11}$$

where $y_0, y_1, y_2, y_3 \in \mathbb{R}$, $f(t)$ is a known function, $m - 1 < \gamma \leq m$, $m \in \mathbb{Z}^+$,$\gamma_0, \gamma_1, \gamma_2, \gamma_3 \leq \gamma$ with the initial states

$$u^{(j)}(0) = c_j \in \mathbb{R}\ , j = 0, 1, ..., m - 1. \tag{12}$$

Approximating

$$D^{\gamma}u(t) \ \text{ as } \ A^T\Psi(t), \text{ we have} \tag{13}$$

$$D^{\gamma_0}u(t) = A^T P^{\gamma-\gamma_0}\Psi(t), \tag{14}$$

$$D^{\gamma_1}u(t) = A^T P^{\gamma-\gamma_1}\Psi(t), \tag{15}$$

$$D^{\gamma_2}u(t) = A^T P^{\gamma-\gamma_2}\Psi(t), \tag{16}$$

$$D^{\gamma_3}u(t) = A^T P^{\gamma-\gamma_3}\Psi(t) \text{ and} \tag{17}$$

$$u(t) = A^T P^\gamma \Psi(t) + \sum_{j=0}^{m-1} u^{(j)}(0) \frac{t^j}{j!}. \tag{18}$$

Similarly, the function $f(t)$ may be expanded by the Chebyshev wavelets as

$$f(t) = F^T \Psi(t), \tag{19}$$

where F^T is a known constant vector.
Using (13-17) and (19) in (11), we attain

$$\begin{aligned} A^T \Psi(t) = y_0 A^T P^{\gamma-\gamma_0} \Psi(t) + y_1 A^T P^{\gamma-\gamma_1} \Psi(t) + y_2 A^T P^{\gamma-\gamma_2} \Psi(t) \\ + y_3 A^T P^{\gamma-\gamma_3} \Psi(t) + F^T \Psi(t), \end{aligned}$$

Since $\Psi(t) = \phi_{\widehat{n}\times\widehat{n}} B_{\widehat{n}}(t)$, we have

$$\begin{aligned} A^T \phi_{\widehat{n}\times\widehat{n}} B_{\widehat{n}}(t) = y_0 A^T P^{\gamma-\gamma_0} \phi_{\widehat{n}\times\widehat{n}} B_{\widehat{n}}(t) + y_1 A^T P^{\gamma-\gamma_1} \phi_{\widehat{n}\times\widehat{n}} B_{\widehat{n}}(t) \\ + y_2 A^T P^{\gamma-\gamma_2} \phi_{\widehat{n}\times\widehat{n}} B_{\widehat{n}}(t) + y_3 A^T P^{\gamma-\gamma_3} \phi_{\widehat{n}\times\widehat{n}} B_{\widehat{n}}(t) + F^T \phi_{\widehat{n}\times\widehat{n}} B_{\widehat{n}}(t). \end{aligned} \tag{20}$$

The equation (20) can be transformed into a system of algebraic equations at

Table 1: Absolute errors of example 6.1 for various values of $\widehat{n}$

t	$\widehat{n} = 24$ $(j = 4, M = 3)$	$\widehat{n} = 48$ $(j = 5, M = 3)$	$\widehat{n} = 96$ $(j = 6, M = 3)$	$\widehat{n} = 192$ $(j = 7, M = 3)$
0.1	5.6757e-04	1.4109e-04	3.5200e-05	8.7901e-06
0.2	5.2023e-04	1.2917e-04	3.2520e-05	8.0929e-06
0.3	4.7091e-04	1.0846e-04	2.4930e-05	6.1988e-06
0.4	1.6459e-05	4.3184e-05	9.2216e-06	1.5083e-06
0.5	5.5512e-03	5.7762e-04	8.1605e-05	1.4377e-05
0.6	1.2675e-03	5.6763e-04	1.4110e-04	3.1709e-05
0.7	5.6379e-03	1.4022e-03	2.9665e-04	7.5132e-05
0.8	8.3151e-03	2.2370e-03	6.5392e-04	1.6275e-04
0.9	2.2315e-02	4.3762e-03	1.1157e-03	2.9777e-04

the collocation points $t_i = \frac{2i-1}{2^j M}, i = 1, 2, ..., 2^{j-1}M$. Solving this system, we can obtain the Chebyshev wavelet co-efficient vector A^T. Then using (18), we get the approximate output response $u(t)$.

In particular, if we choose $\gamma = 2, c_0 = c_1 = 0, y_0 = y_2 = -1, y_1 = 2, y_3 = 0, \gamma_0 = 0, \gamma_1 = 1, \gamma_2 = \frac{1}{2}$ and $f(t) = t^7 + \frac{2048}{429\sqrt{\pi}} t^{6.5} - 14t^6 + 42t^5 - t^2 - \frac{8}{3\sqrt{\pi}} t^{1.5} + 4t - 2$, then the exact solution of (11) is $u(t) = t^7 - t^2$. The absolute errors in Table 1 confirm the convergency and the reliability of the proposed technique.

Example 6.2. In the above example, suppose $\gamma = 2$, $c_0 = c_1 = 0$, $y_0 = y_2 = -1$, $y_1 = 0$, $y_3 = 2$, $\gamma_0 = 0, \gamma_2 = \frac{2}{3} \in (0,1), \gamma_3 = \frac{5}{3} \in (1,2)$,
and
$$f(t) = t^3 + 6t - \frac{12}{\Gamma(\frac{7}{3})} t^{4/3} + \frac{6}{\Gamma(\frac{10}{3})} t^{7/3}.$$

Table 2: Absolute errors of example 6.2 for various values of $\widehat{n}$

t	$\widehat{n} = 24$ $(j = 4, M = 3)$	$\widehat{n} = 48$ $(j = 5, M = 3)$	$\widehat{n} = 96$ $(j = 6, M = 3)$	$\widehat{n} = 192$ $(j = 7, M = 3)$
0.1	1.3231e-03	1.0852e-03	1.0218e-03	1.0057e-03
0.2	9.0992e-03	8.2858e-03	8.0759e-03	8.0200e-03
0.3	2.9622e-02	2.7704e-02	2.7186e-02	2.7049e-02
0.4	6.9620e-02	6.5489e-02	6.4395e-02	6.4103e-02
0.5	1.3600e-01	1.2792e-01	1.2577e-01	1.2520e-01
0.6	2.3717e-01	2.2155e-01	2.1746e-01	2.1638e-01
0.7	3.8203e-01	3.5317e-01	3.4568e-01	3.4370e-01
0.8	5.8250e-01	5.3030e-01	5.1681e-01	5.1326e-01
0.9	8.5504e-01	7.6151e-01	7.3754e-01	7.3123e-01

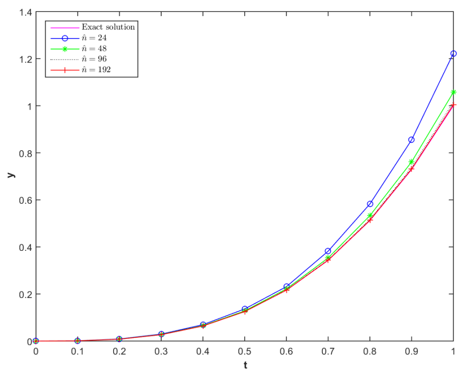

Figure 1: Comparison of Numerical solutions and Exact solutions for example 6.2

The exact solution in this case is $u(t) = t^3$. Table 2 shows that the absolute errors attained by the proposed technique with $M = 3$ and the values of j increasing become smaller and smaller. Figure 1 also depicts the convergency and the reliability of the proposed technique.

Example 6.3. Consider the non-homogeneous multi-order fractional differential equation [13]
$$aD^{\alpha}u(t) + bD^{\beta}u(t) + cu(t) = g(t), \ t \in [0,1), \tag{21}$$

where $a \neq 0,\ b, c \in \mathbb{R}$, $g(t)$ is a known function, $m-1 < \alpha \leq m$, $m \in \mathbb{Z}^+$, $\beta \leq \alpha$ with the initial states $u^{(j)}(0) = u_j \in \mathbb{R},\ j = 0, 1, ..., m-1$.
Now, suppose $\alpha = 2,\ \beta = 0.5,\ a = b = c = 1$, $g(t) = 6t^3\left(\frac{t^{-\alpha}}{\Gamma(4-\alpha)} - \frac{t^{-\beta}}{\Gamma(4-\beta)}\right)$ and $u_0 = u_1 = 0$. Using the proposed technique, we arrive

$$A^T\Psi(t) + A^T P^{0.5}_{\widehat{n}\times\widehat{n}}\Psi(t) + A^T P^{2}_{\widehat{n}\times\widehat{n}}\Psi(t) = G^T\Psi(t).$$

Since $\Psi(t) = \phi_{\widehat{n}\times\widehat{n}}B_{\widehat{n}}(t)$, we have

$$A^T\phi_{\widehat{n}\times\widehat{n}}B_{\widehat{n}}(t) + A^T P^{0.5}_{\widehat{n}\times\widehat{n}}\phi_{\widehat{n}\times\widehat{n}}B_{\widehat{n}}(t) + A^T P^{2}_{\widehat{n}\times\widehat{n}}\phi_{\widehat{n}\times\widehat{n}}B_{\widehat{n}}(t) = G^T\phi_{\widehat{n}\times\widehat{n}}B_{\widehat{n}}(t). \quad (22)$$

The equation (22) can be transformed into a system of algebraic equations at the collocation points. Solving this system, we can attain the co-efficient vector A^T. Maximum absolute errors attained by Legendre wavelets, Haar wavelets and the Chebyshev wavelets are compared in Table 3. Also Table 3 shows that the proposed technique gives better results compared to Haar and Legendre wavelets.

Table 3: Maximum absolute errors of example 6.3 for various values of $\widehat{n}$

	Legendre		Haar		Chebyshev	
β	$\widehat{n}$=24	$\widehat{n}$=96	$\widehat{n}$=32	$\widehat{n}$=128	$\widehat{n}$=32	$\widehat{n}$=128
0.25	8.546×10^{-4}	5.343×10^{-5}	4.807×10^{-4}	3.005×10^{-5}	1.4205×10^{-5}	5.1634×10^{-6}
0.50	7.963×10^{-4}	4.978×10^{-5}	4.479×10^{-4}	2.800×10^{-5}	1.0680×10^{-4}	5.3760×10^{-7}
0.75	7.405×10^{-4}	4.631×10^{-5}	4.166×10^{-4}	2.605×10^{-5}	1.0605×10^{-4}	1.1484×10^{-5}

7. Conclusion

In this paper, an efficient fractional integration operational matrix of the Chebyshev wavelets was derived to attain approximate solutions of multi-order fractional differential equations. Illustrative examples elucidated the solution process, the simplicity and the efficiency of the proposed technique. It is also worth mentioning that the numerical solutions attained by the proposed technique were in a good agreement with the exact solutions.

References

[1] Beylkin G., Coifman R., Rokhlin V., Fast wavelet transforms and numerical algorithms, I. Commun. Pure Appl. Math. 44 (1991), 141-183.

[2] Chang P. and Isah A., Legendre wavelet operational matrix of fractional derivative through wavelet-polynomial transformation and its applications in solving Fractional order Brusselator system, Journal of Physics:Conference Series, 693 2016.

[3] Cong N. D. and Tuan H. T., Generation of nonlocal fractional dynamical systems of fractional differential equations, Journal of integral equations and applications, Vol. 29, No. 4 (2017), 585-608.

[4] Demir A., Bayrak M. A. and Ozbilge E., A New Approach for the Approximate Analytic Solution of Space-Time Fractional Differential Equations by the Homotopy Analysis Method, Advances in Mathematical Physics, (2019), Article ID.5602565.

[5] Ge F., Chen Y. Q., Kou C. and Podlubny I., On the regional controllability of the sub-diffusion process with Caputo fractional derivative, Fractional Calculus and Applied Analysis, Vol. 19, No. 5, (2016).

[6] Han W., Chen Yi-Ming, Liu Da-Yan, Xiao-Lin, Boutat D., Numerical solution for a class of multi-order fractional differential equations with error correction and convergence analysis, Advances in Difference equations, 253 (2018).

[7] Jajarmi A., Hajipour M., Mohammadzadeh E., Baleanu D., A new approach for the nonlinear fractional optimal control problems with external persistent disturbances, J. Franklin Inst., 355 (9) (2018), 3938-3967.

[8] Javeed S., Baleanu D., Waheed A., Khan M. S. and Affan H., Analysis of homotopy perturbation method for solving fractional order differential equations, Mathematics, 7 (1) (2019), 40.

[9] Keshavarz E., Ordokhani Y., Razzaghi M., The Bernoulli wavelets operational matrix of integration and its applications for the solution of linear and nonlinear problems in Calculus of variations, Applied Mathematics and Computation, Vol. 351 (2019), 83-98.

[10] Kilicman A., Kronecker operational matrices for fractional calculus and some applications, Appl. Math. Comput. 187 (2007), 250-265.

[11] Li W., Pang Y., Application of Adomian decomposition method to non-linear systems, Advances in Difference Equations, 67 (2020).

[12] Ma Y., Li W., Application and research of fractional differential equations of dynamic analysis of supply chain financial chaotic system, Chaos, Solitons and Fractals, 130 (2020).

[13] Rehman M., Khan R. A., The Legendre wavelet method for solving fractional differential equations, Commun Nonlinear Sci Numer Simulat, 16 (2011), 4163-4173.

[14] Wang Y., Yin T., Sine-Cosine wavelet operational matrix of fractional order integration and its applications in solving the fractional order Riccati differential equations, Advances in Difference Equations, 222 (2017).

[15] Wang Y., Zhu Li and Wang Zhi, Solving the nonlinear variable order fractional differential equations by using Euler wavelets, CMES, Vol. 118, No. 2 (2019), 339-350.

[16] Xie J., Wang T., Ren Z., Zhang J. and Quan L., Haar wavelet method for approximating the solution of a coupled system of fractional-order integral-differential equations, Mathematics and Computers in simulation, 163 (2019), 80-89.

[17] Ziane D., Cherif M. H., Variational iteration transform method for fractional differential equations, Journal of Interdisciplinary Mathematics, Vol. 21, No.1 (2018), 185-199.